19th Brazilian Congress of Thermal Sciences and Engineering
November 06th-10th, 2022, Bento Gonçalves - RS - Brazil

# ENC-2022-0490
# COOLING BY MIXED CONVECTION OF A HEATED OBSTACLE IN A LID-DRIVEN CAVITY OF DIFFERENT ASPECT RATIOS: A CONSTRUCTAL DESIGN STUDY

**Rafael da Silveira Borahel**
Mechanical Engineering Graduate Program, Universidade do Vale do Rio dos Sinos, 93022-750, São Leopoldo, RS, Brazil
rborahel@edu.unisinos.br

**Flávia Schwarz Franceschini Zinani**
Mechanical Engineering Graduate Program, Universidade do Vale do Rio dos Sinos, 93022-750, São Leopoldo, RS, Brazil
fzinani@unisinos.br

**Luiz Alberto Oliveira Rocha**
Mechanical Engineering Graduate Program, Universidade Federal do Rio Grande do Sul, 90040-001, Porto Alegre, RS, Brazil
Computational Modeling Graduate Program, Universidade Federal do Rio Grande, 96203-900, Rio Grande, RS, Brazil
luizrocha@mecanica.ufrgs.br

***Abstract.*** *The main purpose of this study is to maximize the dimensionless heat transfer rate (q*) between a heated block (HB) and the surrounding fluid flow in a two-dimensional lid-driven cavity. The constraints of the problem are the cavity area (A) and the HB aspect ratio (AR), while the Degree of Freedom (DOF) is the cavity aspect ratio (AR). The effects of Richardson Number (Ri) and the area fraction between the HB and the cavity areas ($\phi$) are also explored. The air convective flow is laminar, incompressible, and steady-state. The mathematical model is based on the balance equations of mass, momentum and energy. The finite volume method is used to numerically solve the problem. The grid meshes employed in the spatial discretization are subjected to uncertainty analysis using the GCI method, while the mathematical and numerical models are verified against other studies available in the literature. For all Ri and $\phi$ tested, the results indicate that the heat transfer is enhanced by low AR, especially AR = 0.5, which have an elongated horizontal shape. For this AR, the highest q* (19.22) is obtained when the forced convection (Ri = 0.1) prevails and the biggest HB ($\phi$ = 1/4) is tested.*

***Keywords:*** *constructal design, heat transfer in enclosure, lid-driven cavity, mixed convection.*

## 1. INTRODUCTION

Internal flow with heat transfer in lid-driven cavities is considered a classic engineering problem. In these systems, two different mechanisms are responsible for the heat transfer: forced convection (related to the shear forces produced by the lid-driven surface's movement) and natural convection (caused by the buoyancy flow generated by the temperature gradients). If both mechanisms have the same importance, the heat transfer inside the cavity occurs by mixed convection (Razera et al., 2018; Gangawane et al., 2019; Rodrigues et al., 2020). This phenomenon is found in various practical applications – like nuclear reactors, solar power collectors, solar ponds, furnace, metal coating, float grass production, crystal growth, drying technology and food processing – but it draws attention mainly in the electronic device cooling (Al-Amiri and Khanafer, 2011; Nithyadevi et al., 2013). Seeking to understand how the mixed convection can be used to promote the thermal control of enclosed gadgets, studies involving cooling of heated obstacles inside lid-driven cavities have gained importance in the last decade. Gangawane (2017) investigated the role of Prandtl (*Pr*) and Grashof (Gr) numbers in the convective heat tranfer of a triangular obsctacle inside a lid-driven cavity. According to the author, some bifurcations in the fluid flow are observed when natural convection is dominant ($Gr \geq 10^3$) due to the fluid motion from the heated triangular surfaces towards the vertical ambient wall. The effects of size and location of a heated tringular block inside a square lid-driven cavity are adressed by Gangawane et al. (2018). Based on theirs results, Gangawane et al. (2018) state that the heat transfer was maximized when the largest blocks tested were centralized in the cavity. Investigations regarding the role of the obstacle size are also related by Islam et al. (2012), but for an obstacle with square shape. In this study, the obstacle size affected the heat transfer in a different form depending on the convection regime.

For the forced and mixed convection regimes, the largest block intensified the average Nusselt numbers ($\overline{Nu}$) in the obstacle surfaces. However, the smallest block proved to be the better option when the natural convection prevails. In all studies mentioned, as well as in other existing in the literature, it is proven that the geometric characteristics of the cavity and the obstacle play a relevant role in the fluid dynamics and heat transfer of the flow. Thus, techniques/methods suitable for the study of designs/geometries and their effects on the processes in which they act are interesting for this kind of problem, such as the constructal design method.

This method has been used to study the design in flow systems following the constructal law principle, that affirms: a finite flow system, animate or inanimate, only persists in time (survives) if its configuration changes to provide easier access to its internal streams [fluid, energy, species, etc] (Bejan and Lorente, 2008). Based on constraints (geometrical or physical) and objectives (performance indicators), the constructal design method can be considered a tool capable of maximizing or minimizing the performance indicators of systems in different areas through the analysis of their designs. Building safety (Lui et al., 2015), medicine (Dutra et al., 2021), solar air heaters (Barik et al., 2021) and thermal energy storage systems (Joshi and Rathod, 2019) are examples of areas where the method has been successfully applied, proving its multidisciplinary character.

Using the constructal design method, the present numerical work aims to improve the convective heat transfer between an isothermal heated block (HB) and the surrounding air flow in an unstable top lid-driven cavity. The cavity aspect ratio ($AR$ = 0.5, 1.0, 1.5 and 2.0) is adopted as the Degree of Freedom (DOF), while the effects of $Ri$ (0.1, 1.0 and 10) and the area fraction between HB and the cavity areas (1/4, 1/8, 1/16, and 1/32) are also explored. Considering all parameters tested, 36 different configurations for the cavity and the flow are analyzed in this work.

## 2. PROBLEM DESCRIPTION

As already mentioned, the convective heat transfer between an isothermal HB and the surrounding flow (air) in an unstable top lid-driven cavity is numerically investigated here. Figure 1 shows the schematic representation of the two-dimensional computational domain.

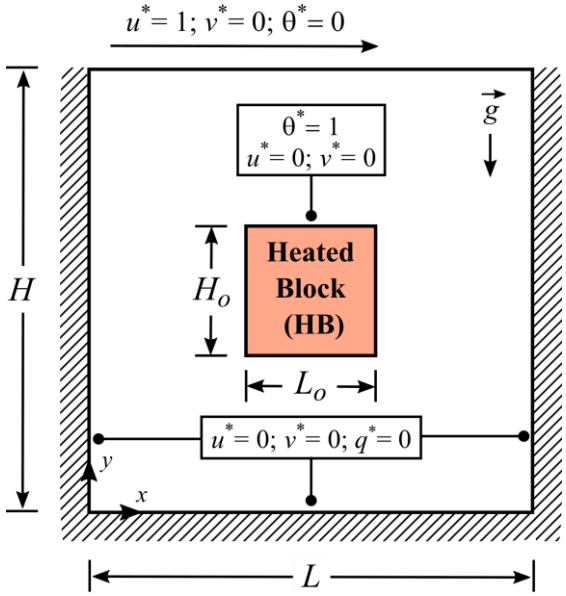


Figure 1. Schematic representation of the computational domain.

In order to promote the heat transfer between the HB and the working fluid, the constructal design method was applied to find out which geometric and flow configurations are the most appropriate for this purpose. The performance parameter to be maximized is the dimensionless heat transfer rate ($q^*$), given by $q^* = (q/k.W.\Delta T)$, where $q$ is the heat transfer rate at the HB surfaces, $W$ is the unitary cavity depth and $\Delta T$ is the difference between the HB ($T_{HB}$) and the lid-driven surface ($T_{lid}$) temperatures. The geometric constraints are the cavity area ($A=H.L$) and the HB aspect ratio ($AR_o=H_o/L_o$ = 1), while the cavity aspect ratio (AR=$H/L$ = 0.5, 1.0, 1.5 and 2.0) is the degree of Freedom (DOF) of the problem, where: $H$ and $L$ are the cavity height and length and $H_o$ and $L_o$ the HB height and length. In addition to $AR$, the effects of Richardson number ($Ri = Gr/Re^2$) and area fraction between HB and cavity areas ($\phi$ = 1/4, 1/8, 1/16 and 1/32) are also investigated. $Gr_{\sqrt{A}}$ is the Grashof number [Eq. (1)] which in this work assumes a fixed value of $10^5$ and $Re_{\sqrt{A}}$ is the Reynolds number [Eq. (2)] which value is varied to obtain $Ri$ = 0.1, 1.0 and 10 (forced, mixed and natural convection regime).

$$Gr_{\sqrt{A}} = \frac{\vec{g}\beta\Delta T\sqrt{A}^3}{\nu^2} \tag{1}$$

$$Re_{\sqrt{A}} = \frac{U_{lid}\sqrt{A}}{\nu} \tag{2}$$

where $U_{lid}$ is the lid wall velocity, $\vec{g}$ is the gravity acceleration and $\nu$ is the kinematic viscosity of the air.

For a better understanding of all aspects involved in the application of the constructal design method in the present study, a flowchart that explains the mains steps followed here to apply the method is presented in Fig 2.

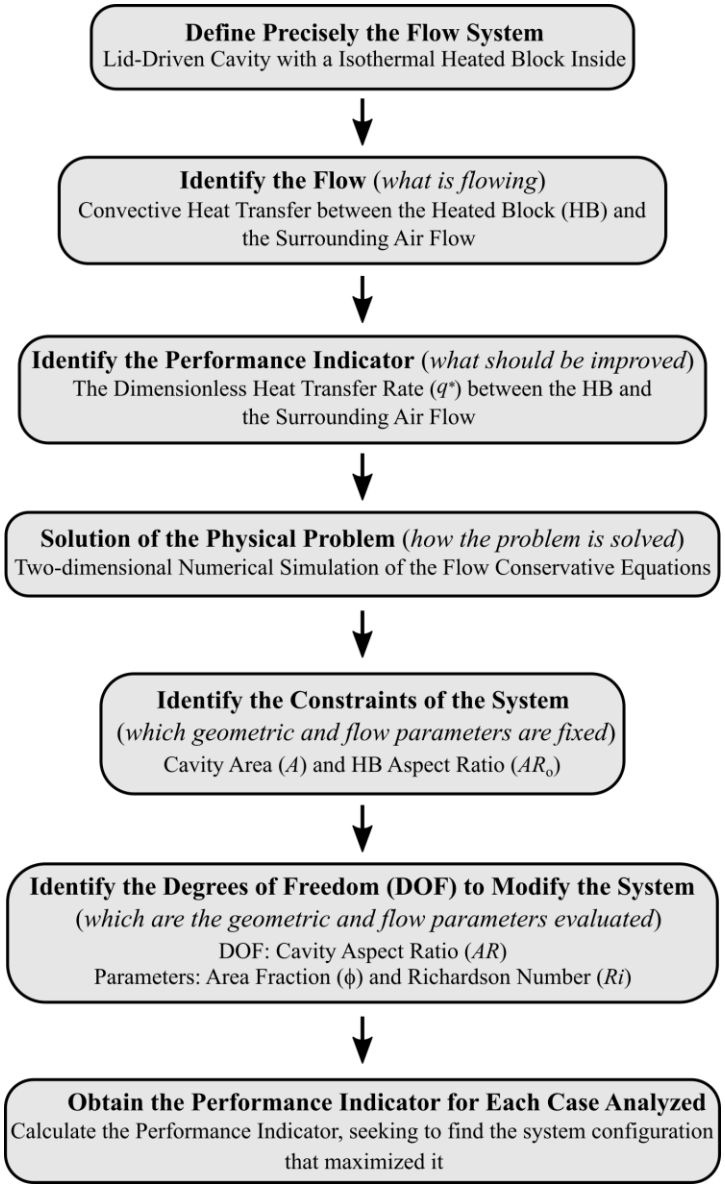


Figure 2. Flowchart with the main steps followed in this work to apply the constructal design method.

### 2.1 Mathematical Model

For this problem, the two-dimensional mathematical model is composed by the conservation equations of mass, momentum (in *x* and *y* directions) and energy (Bejan, 2013), respectively described by Eqs. (3-6). The flow is considered laminar, incompressible and steady-state. All thermophysical properties of the air are kept constant, with the exception of

density ($\rho$), which is treated as a function temperature by the Boussinesq approximation in the buoyancy term of the momentum equation.

$$\frac{\partial u}{\partial x}+\frac{\partial v}{\partial y}=0 \tag{3}$$

$$\rho\left(u\frac{\partial u}{\partial x}+v\frac{\partial u}{\partial y}\right)=-\frac{\partial p}{\partial x}+\mu\left(\frac{\partial^2 u}{\partial x^2}+\frac{\partial^2 u}{\partial y^2}\right) \tag{4}$$

$$\rho\left(u\frac{\partial v}{\partial x}+v\frac{\partial v}{\partial y}\right)=-\frac{\partial p}{\partial y}+\mu\left(\frac{\partial^2 v}{\partial x^2}+\frac{\partial^2 v}{\partial y^2}\right)+\rho\vec{g}\beta(T-T_r) \tag{5}$$

$$\rho c_p\left(u\frac{\partial T}{\partial x}+v\frac{\partial T}{\partial y}\right)=k\left(\frac{\partial^2 T}{\partial x^2}+\frac{\partial^2 T}{\partial y^2}\right) \tag{6}$$

where $x$ and $y$ are the Cartesian coordinates in the horizontal and vertical directions, $u$ and $v$ are the flow velocities in the horizontal and vertical directions, $\mu$ is the dynamic viscosity, $p$ is the pressure, $\vec{g}$ is the gravity acceleration, $\beta$ is the thermal expansion coefficient, $T$ is the temperature, $Tr$ is the reference temperature, $c_p$ is the specific heat and $k$ is the thermal conductivity.

To generalize the problem and its results, the dimensionless forms of the geometric and flow parameters, i.e., Cartesian coordinates ($x$ and $y$), cavity ($H$ and $L$), and HB ($H_o$ and $L_o$) dimensions, are adopted as follows, respectively:

$$x^*, y^*, H^*, L^*, H_o^*, L_o^* = \frac{x, y, H, L, H_o, L_o}{\sqrt{A}} \tag{7}$$

$$u^*, v^* = \frac{u, v}{U_{lid}} \tag{8}$$

$$\theta^* = \frac{T-T_{lid}}{T_{HB}-T_{lid}} \tag{9}$$

where $x^*$ and $y^*$ are the dimensionless Cartesian coordinates in the horizontal and vertical directions, $u^*$ and $v^*$ are the dimensionless flow velocities in the horizontal and vertical directions and $\theta^*$ is the dimensionless temperature.

#### 2.1.1 Boundary Conditions

As already shown in Fig. 1, the non-slip condition ($u^* = v^* = 0$) was applied to all stationary walls (cavity and HB), while a constant rightward velocity ($u^* = 1$) is prescribed to the moving wall. The adiabatic condition ($q^* = 0$) was adopted in the bottom, left, and right walls of the cavity, the lowest temperature ($\theta^* = 0$) in the moving surface and the highest temperature ($\theta^* = 1$) in the HB walls.

### 2.2 Numerical Model

In the present work, numerical simulations – based in the finite volume method (FVM) – were employed to solve the proposed problem. All numerical simulations were carried out in the commercial software ANSYS Fluent 2021 R1, using a pressure-based solver. The SIMPLE algorithm was applied to solve the pressure-velocity coupling, PRESTO! scheme for the pressure interpolation, *Least Squares Cell-Based* for the gradient discretization and *Second-Order Upwind* for the advective terms of momentum and energy equations. As convergence criteria of the conservation equations, a residual of $10^{-6}$ was adopted for the mass and momentum, while $10^{-8}$ was assumed to the energy.

#### 2.2.1 Mesh Quality Analysis

Two-dimensional grid meshes of quadrilateral cells were applied in the spatial discretization of the computational domain. In the regions where the largest velocity and temperature gradients occur - close to the cavity and HB walls –

more cells were used, configuring a mesh refinement in these regions. The mesh quality analysis was carried out employing the GCI (*GridConvergence Index*) method (Celik et al., 2008). To apply the method, three meshes with different quantities of cells (66.300, 38.740, 22.860) - named M1, M2, and M3, respectively – were generated and tested in the computational domain of a critical case ($\phi$ = 1/4, $AR$ = 0.5, $Ri$ = 0.1). For the analysis, three control parameters were considered to assess the numerical uncertainty between the meshes: $v^*_{min}$ and $v^*_{max}$ at $H^*$ = 0.5 and $q^*$. The numerical uncertainties between M1 and M2 ($GCI_{21}$) and M2 and M3 ($GCI_{32}$) were, respectively, 0.31 % and 0.19 % for $v^*_{min}$, 0.09 % and 0.02 % for $v^*_{max}$ and 0.009 % and 0.008 % for $q^*$. Therefore, considering the small uncertainties verified through the GCI method, it can be affirmed that the M1 mesh (shown in Fig. 3) has an adequate quality for the spatial discretization of the problem, so that all the other meshes were built from its parameters.

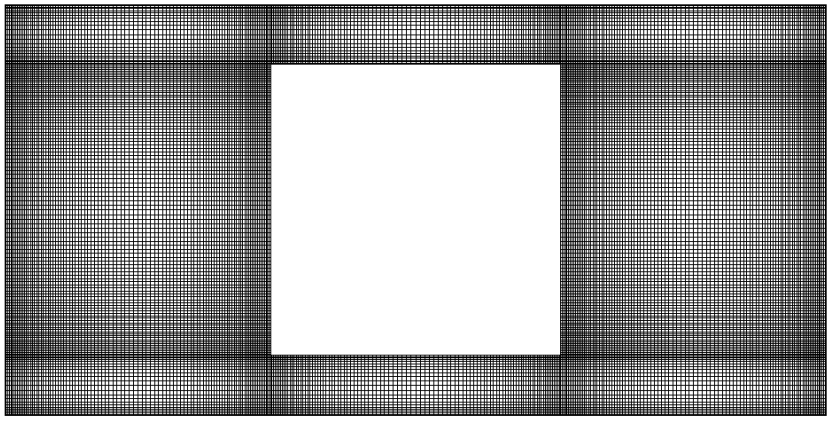

Figure 3. Grid mesh of the cavity with $\phi$ = XX and $AR$ = XX.

### 2.2.2 Model Verification

To ensure that the mathematical and numerical model is appropriate for the proposed problem, the studies of Islam et al. (2012) and Moraga et al. (2017) were reproduced for verification purposes. In both studies, a heated obstacle is cooled inside a cold-walled lid-driven cavity for $Ri$ = 0.1, 1.0 and 10; problems similar to the one studied here. The $u^*$ and $v^*$ profiles, at the vertical and horizontal mid-planes ($L^*$ = 0.5 and $H^*$ = 0.5, respectively) of the cavities, from Islam et al. (2012), Moraga et al. (2017) and present work are shown in the Fig. 4 (a-c), where (a) $Ri$ = 0.1, (b) $Ri$ = 1.0 and (c) $Ri$ = 10.

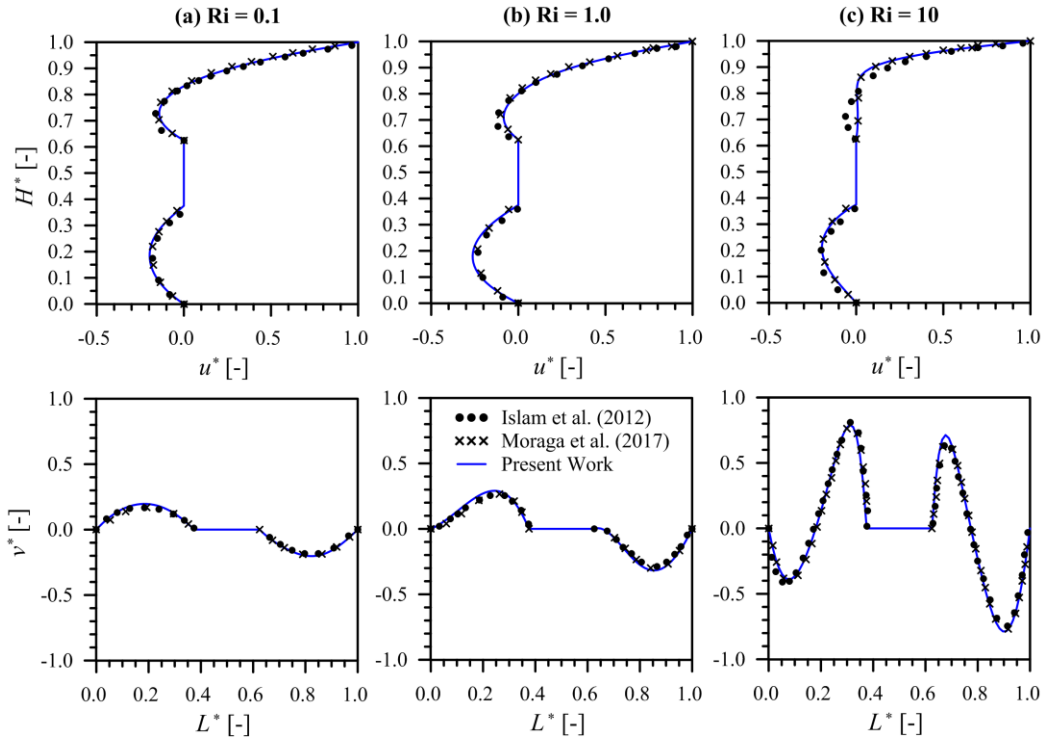

Figure 4. $u^*$ and $v^*$ profiles, at $L^* = 0.5$ and $H^* = 0.5$, obtained from Islam et al. (2012), Moraga et al. (2017) and present work, where: (a) $Ri = 0.1$, (b) $Ri = 1.0$ and (c) $Ri = 10$.

As can be seen, a great similarity between all the numerical results exists for $Ri = 0.1$ and 1.0, respectively, Fig. 4 (a-b). However, some differences - between Islam et al. (2012) and present work - are observed for $u^*$ (in $0.65 \leq H^* \leq 0.9$), when $Ri = 10$ [Fig. 4 (c)]. Despite these differences, the results obtained here are very still similar to those presented by Moraga et al. (2017), which proves that the mathematical and numerical model can satisfactorily reproduce the velocity profiles of the working fluid inside the cavity. Regarding the thermal issues of the problem, Tab. 1 presents the average Nusselt number ($\overline{Nu}_{\sqrt{A}}$) at HB walls, obtained by Islam et al. (2012) and present work, using $\overline{Nu}_{\sqrt{A}} = (q''.\sqrt{A}) / (k.\Delta T)$; where $q''$ is the heat flux at HB surfaces.

Table 1. $\overline{Nu}_{\sqrt{A}}$ at HB surfaces from Islam et al. (2012) and present work.

| | $\overline{Nu}_{(Ri=0.1)}$ | $\overline{Nu}_{(Ri=1.0)}$ | $\overline{Nu}_{(Ri=10)}$ |
|---|---|---|---|
| Islam et al. (2012) | 5.57 | 5.70 | 7.98 |
| Present Work | 5.56 | 5.60 | 7.97 |
| $\Delta\overline{Nu}$ (%) | 0.18 | 1.78 | 0.12 |

According to the results presented in Tab. 1, it can be affirmed that the values of $\overline{Nu}_{\sqrt{A}}$ obtained here are very similar to those reported by Islam et al. (2012). The largest percentage difference are related to the $Ri$ =1.0 case, where the difference between the results is equal to 1.78%. For the other cases, where the convection regime is forced ($Ri = 0.1$) or natural ($Ri = 10$), $\Delta\overline{Nu}$ is 0.18 % and 0.12 %, respectively. Thus, analyzing together $\overline{Nu}_{\sqrt{A}}$ and the velocities profiles, it is possible to say that the mathematical and numerical model is adequate for the proposed study.

## 3. RESULTS AND DISCUSSIONS

The $AR$ and $\phi$ effects on the dimensionless heat rate ($q^*$) inside the cavity are presented in Fig. 5 for the different convection regimes (forced, natural and mixed) tested, respectively, (a) $Ri = 0.1$, (b) $Ri = 1$ and (c) $Ri = 10$.

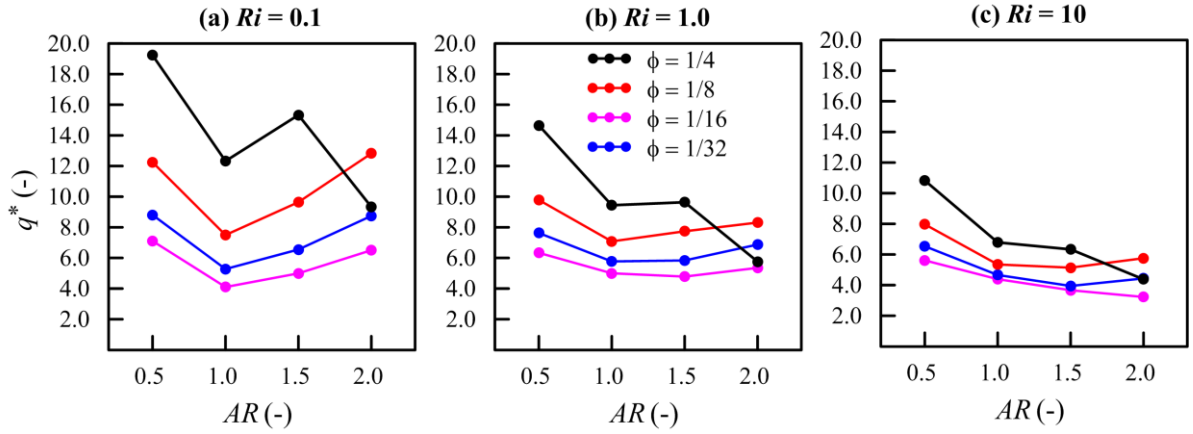


Figure 5. $AR$ and $\phi$ effects on the dimensionless heat rate ($q^*$) inside the cavity, where: (a) $Ri = 0.1$, (b) 1.0 and (c) 10.

As can be seen in Fig. 5 (a-c), $q^*$ proved to be proportional to $\phi$ for practically all $AR$. It can be explained by the heat transfer area of the HB, which increases with $\phi$ and, consequently, enhances $q^*$ between the HB and the surrounding air flow. However, this behavior is not fully valid for $AR = 2.0$, where $\phi$ = 1/8 and 1/16 demonstrated to be better options to promote the heat transfer in some cases. For $AR = 2.0$ and $Ri = 0.1$ [Fig. 5 (a)], $q^*$ is 37.4% greater when $\phi = 1/8$ is adopted instead of $\phi$ = 1/4. For the same $AR$, but $Ri = 1.0$ [Fig. 5 (b)], $q^*_{(\phi = 1/8)}$ is 44.3% higher than $q^*_{(\phi = 1/4)}$, while $q^*_{(\phi = 1/16)}$ is 19.4% greater. This superiority also is observed for $AR = 2.0$ and $Ri = 10$ [Fig. 5 (c)], but less intensely, once $q^*_{(\phi = 1/8)}$ and $q^*_{(\phi = 1/16)}$ are, respectively, 31.5% and 1.3% superior to $q^*_{(\phi = 1/4)}$. This behavior suggests that larger HBs, although intensifying $q^*$ due to their heat exchange area, may in some situations not be the most beneficial, probably because they act as a difficult obstacle to be overcome by the fluid flow. Analyzing the $AR$ effects, it is evident that $q^*$ is maximized when the cavity has a horizontal shape ($AR = 0.5$). This observation is valid for all cases, with the exception of one [$\phi = 1/8$ and $Ri = 0.1$], where the highest $q^*$ (12.8) was obtained with $AR = 2.0$ instead $AR = 0.5$. The fact that $q^*$ is enhanced by $AR = 0.5$ is directly linked to the momentum of the fluid. As the cavity takes a horizontal shape with $AR = 0.5$, the moving wall is larger, so the fluid momentum is greater, which intensifies the convection inside the cavity. However,

the *AR* effects are not dependent on a single factor, but rather on a set of factors. If the *AR* effects were related only to fluid momentum variations, a gradual reduction of $q^*$ would be observed with the increase of *AR*, which is observed only for two cases ($\phi$ = 1/4 and $\phi$ = 1/16) in Fig. 5 (c). This suggests that changes in the flow occur inside the cavity when the *AR* is modified, which affect the heat transfer, similarly to what has already been observed and discussed for $\phi$. Regarding *Ri*, it is possible to affirm that $q^*$ is improved by *Ri* = 0.1 (forced convection), followed by *Ri* = 1.0 and 10. For $\phi$ = 1/4 and *AR* = 0.5, $q^*_{(Ri = 0.1)}$ is 31.2% greater than $q^*_{(Ri = 1.0)}$ and 77.5% if compared to $q^*_{(Ri = 10)}$. Considering all cases, the most pronounced $q^*$ (19.2) is observed when the following cavity and flow parameters are adopted together: $\phi$ = 1/4, *AR* = 0.5 and *Ri* = 0.1 [first point of the black line in Fig. 5 (a)].

The Fig. 6 (a-c) presents the dimensionless heat rate ($q^*$) in each HB wall for (a) *Ri* = 0.1, (b) *Ri* = 1 and (c) *Ri* =10, where (i) $\phi$ = 1/4, (ii) $\phi$ = 1/8, (iii) $\phi$ = 1/16 and (iv) $\phi$ = 1/32.

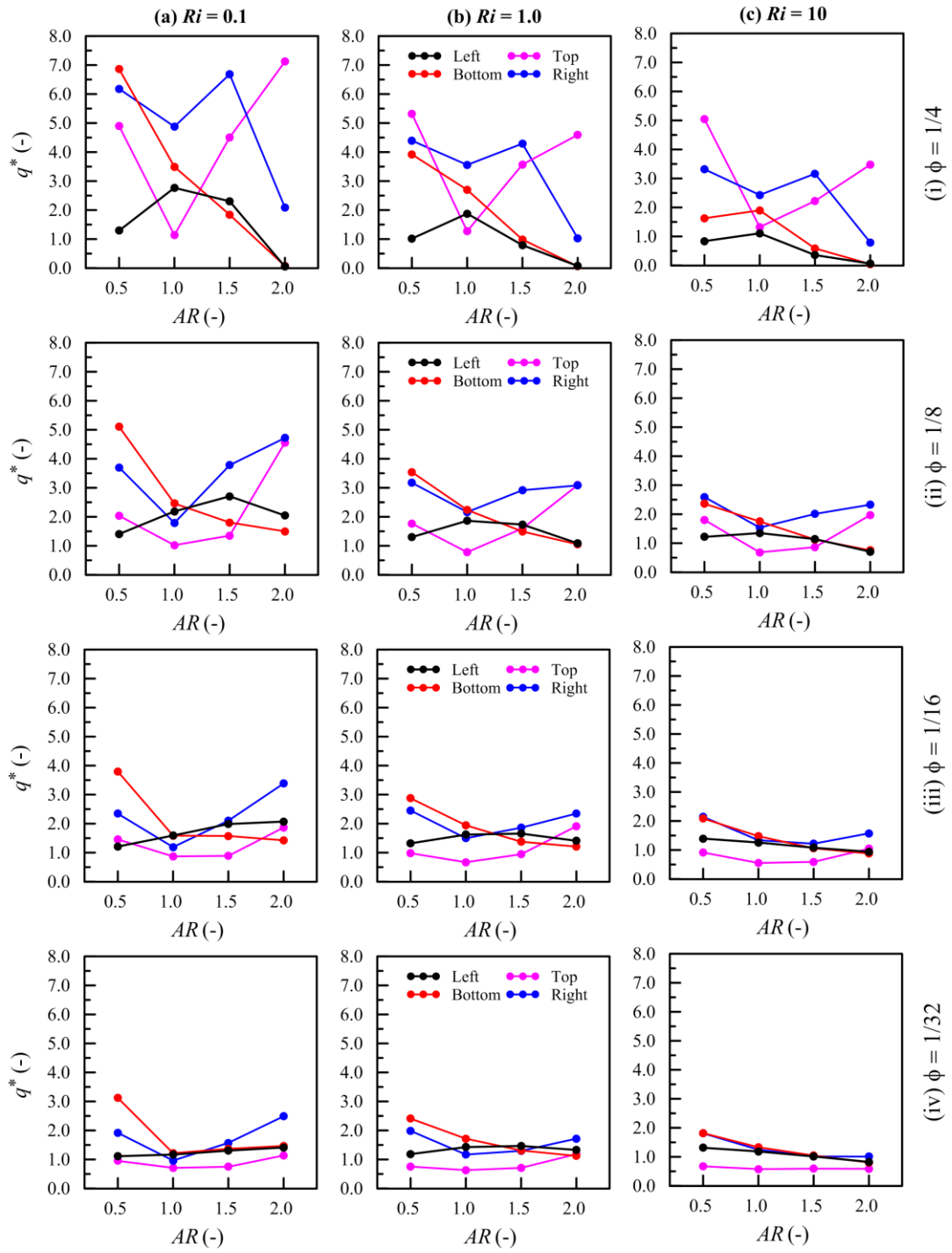


Figure 6. $q^*$ *vs. AR* in each HB wall for (a) *Ri* = 0.1, (b) 1.0 and (c) 10, where (i) $\phi$ = 1/4, (ii) $\phi$ = 1/8, (iii) $\phi$ = 1/16 and (iv) $\phi$ = 1/32.

Analyzing Fig. 6 (a) (i), it is evident the reasons why $q^*_{max}$ is related to the case where the forced convection ($Ri$ =0.1) is employed together $\phi$ = 1/4 and $AR$ = 0.5. In this figure, it is possible to note that the heat transfer on the HB walls, with the exception of the left wall, occurs intensely when $AR$ = 0.5 is adopted. As the total dimensionless heat rate of the HB is given by the sum of $q^*$ at each of its walls, it can be stated that the flow pattern formed inside the cavity in this case is adequate to promote the heat transfer, once it intensified the heat exchange in three walls to the detriment of one. An opposite behavior is observed in the same figure [Fig. 6 (a) (i)] for $AR$ = 2.0. In this case, there is the intensification of $q^*$ in one HB wall (top wall) to the detriment of the others, especially in the right and bottom HB walls. In these walls, $q^*$ is practically null, suggesting the absence of relevant flow close to them, so that the heat transfer occurs almost exclusively by diffusion. These behaviors - observed for $AR$ = 0.5 and 2.0 when the forced convection ($Ri$ =0.1) prevails - are also valid for $Ri$ = 1.0 and 10 [Fig. 6 (a) (ii-iii)], which explains $q^*_{min}$ and $q^*_{max}$ related to $\phi$ = 1/4 in Fig. 5 (a-c). Some universal behaviors, valid for all cases independently of $\phi$ and $Ri$, can be noticed in a broader analysis of Fig. 6. Optimized heat transfer at bottom HB wall - when $AR$ = 0.5 (except for $\phi$ = 1/4 and $Ri$ = 10) - or attenuated at top HB wall - when $AR$ = 1.0 - are examples of the general behaviors. However, for a deep understanding of the peculiarities of the problem, individual analyzes of each case through temperature contours and velocity vectors are necessary.

Figure 7 (a-b) introduces the dimensionless temperature contours and velocity vectors of the $\phi$ = 1/4 case for $Ri$ = 0.1, where (a) $AR$ = 0.5 and (b) $AR$ = 2.0.

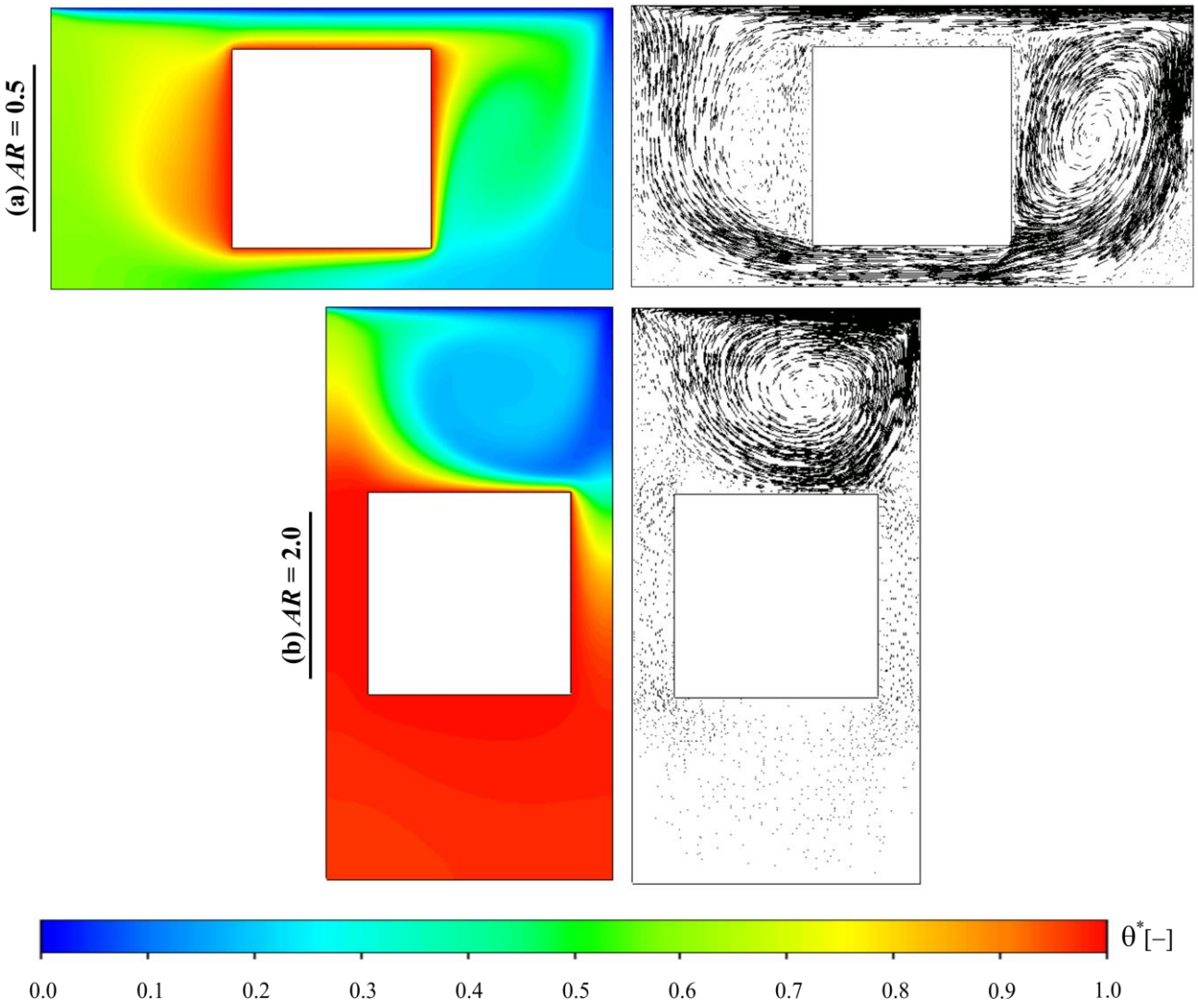


Figure 7. Dimensionless temperature contours and velocity vectors of the $\phi$ = 1/4 case for $Ri$ = 0.1, where (a) $AR$ = 0.5 and (b) $AR$ = 2.0.

In the velocity vectors shown in Fig. 7, it can be seen – for both cases - that the fluid in the upper region of the cavity moves to the right inducted by the shear forces created by the moving wall. This parcel of fluid collides with the right wall of the cavity and adopts a downward movement slightly inclined to the left. For $AR$ = 0.5 [Fig. 7 (a)], the right channel of flow (space between the HB and right wall of the cavity) has an expressive size, which allows the downward

movement of the fluid towards the lower right corner of the HB. In this location, the fluid flow is divided into two parcels: ***i*)** one that collides with the HB and takes an upward movement that gives rise to a convective cell that occupy the entire right channel of flow and ***ii***) another that enters into the lower channel of flow and moves towards the left region of the cavity. This flow pattern is beneficial for the heat transfer, as already verified in Fig. 5 (a) and now pointed out by the absence of hot spots on the dimensionless temperature contour shown in Fig. 7 (a). On the other hand, the fluid flow for $AR = 2.0$ it is restricted to the top region of the cavity, as can be seen in Fig. 7 (b). As in this case, the right channel of flow has a smaller size and the fluid adopts a downward movement slightly inclined to the left after colliding with the right wall of the cavity; the fluid flow instead of descending into the channel ends up colliding in the top wall of the HB. Due to this behavior, a convective cell is created at top of the cavity, while the flow is negligible in the other regions. Thus, the fluid is not "renewed" in these regions, which leads to its heating and consequent drop in the heat transfer; exactly what is observed in the dimensionless temperature contour shown in Fig. 7 (b) and the behavior of $q^*$ in Figs. 5-6 (a).

## 4. CONCLUSIONS

Using the constructal design method, the present study aimed to improve the convective heat transfer between an isothermal heated block (HB) and the surrounding air flow in an unstable top lid-driven cavity. The cavity aspect ratio (*AR*) was adopted as the Degree of Freedom (DOF) of the problem, while the effects of Richardson number (*Ri*) and the area fraction between HB and the cavity areas ($\phi$) were also explored. The proposed problem was analyzed using numerical simulations based in the finite volume method (FVM). The computational domain was considered two-dimensional, while the fluid flow was adopted as laminar, incompressible and steady-state. Based on the results obtained for each of the 36 different configurations tested for the cavity, the following conclusions were drawn:

**i)** The dimensionless heat transfer rate ($q^*$) proved to be proportional to $\phi$. It can be explained by the heat transfer area of the HB, which increases with $\phi$ and, consequently, enhances $q^*$. However, this behavior is not fully valid for all cases, since in some situations $\phi = 1/8$ and 1/16 demonstrated to be better options to promote the heat transfer instead of $\phi = 1/4$. This behavior suggests that larger HBs, although intensifying $q^*$ due to their heat exchange area, may in some situations not be the most beneficial, because they act as a difficult obstacle to be overcome by the fluid flow.

**ii)** For all cases - with the exception of one ($\phi = 1/8$ and $Ri = 0.1$) - $q^*$ was maximized when the cavity adopted a horizontal shape ($AR = 0.5$). This behavior is directly linked to the momentum of the fluid. As the moving wall is larger when the horizontal shape is adopted, the fluid momentum is greater, which results in the intensification of the convection. However, the results also suggest that changes in the flow pattern occur inside the cavity when the *AR* is modified. Thus, it can be affirmed that the AR effects are caused by two factors: variations in the momentum of the fluid and in its flow pattern.

**iii)** Regarding *Ri*, it is possible to affirm that $q^*$ is inversely proportional to it. In this work, $q^*$ was improved by $Ri = 0.1$ (forced convection), followed by $Ri = 1.0$ and 10. Considering all cases, the most pronounced $q^*$ (19.2) is observed when the following cavity and flow parameters were adopted together: $\phi = 1/4$, $AR = 0.5$ and $Ri = 0.1$.

## 5. ACKNOWLEDGEMENTS

The authors acknowledge the agencies CAPES, CNPq, FAPERGS (Proc. No. 311444/2021-0) and the UNISINOS Academic Research and Postgraduate Unit. R.S. Borahel has a doctorate degree scholarship financed by CAPES (Code 001). F.S.F. Zinani is a grant holder of CNPq (Proc. No. 311444/2021-0). L.A.O. Rocha is a grant holder of CNPq (Proc. No. 307791/2019-0).

## 6. REFERENCES

Al-Amiri, A. and Khanafer, K., 2011. "Fluid–structure interaction analysis of mixed convection heat transfer in a lid-driven cavity with a flexible bottom wall". *International Journal of Heat and Mass Transfer*, Vol. 54, pp. 3826–3836.

Barik, A., Mohanty, A., Senapati, J.R. and Awad, M.M., 2021. "Constructal design of different ribs for thermo-fluid performance enhancement of a solar air heater (SAH)". *International Journal of Thermal Sciences*, Vol. 160.

Bejan, A., 2013. *Convection Heat Transfer*. John Wiley & Sons, New Jersey.

Bejan, A. and Lorente, S., 2008. *Design with Constructal Theory*. John Wiley & Sons, New Jersey.

Celik, I.B., Ghia, U., Roache, P.J., Freitas, C.J., Coleman, H., Raad, P.E., 2008. "Procedure for estimation and reporting of uncertainty due to discretization in CFD applications". *Journal of Fluids Engineering*, Vol. 130.

Dutra, R.F., Zinani, F.S.F., Rocha, L.A.O. and Biserni, C., 2021. "Effect of non-Newtonian fluid rheology on an arterial bypass graft: A numerical investigation guided by constructal design". *Computer Methods and Programs in Biomedicine,* Vol. 201, pp. 105944.

Gangawane, K.M., 2017. "Computational analysis of mixed convection heat transfer characteristics in lid-driven cavity containing triangular block with constant heat flux : Effect of Prandtl and Grashof numbers". *International Journal of Heat and Mass Transfer,* Vol. 105, pp. 34–57.

Gangawane, K.M., Oztop, H.F. and Abu-Hamdeh, N., 2018. "Mixed convection characteristic in a lid-driven cavity containing heated triangular block: Effect of location and size of block". *International Journal of Heat and Mass Transfer,* Vol. 124, pp. 860–875.

Gangawane, K.M., Oztop, H.F. and Ali, M.E., 2019. "Mixed convection in a lid-driven cavity containing triangular block with constant heat flux: Effect of location of block". *International Journal of Mechanical Sciences,* Vol. 152, pp. 492–511.

Islam, A.W., Sharif, M.A.R. and Carlson, E.S., 2012. "Mixed convection in a lid driven square cavity with an isothermally heated square blockage inside". *International Journal of Heat and Mass Transfer,* Vol. 55, pp. 5244-5255.

Joshi, V. and Rathod, M.K., 2019. "Constructal enhancement of thermal transport in latent heat storage systems assisted with fins". *International Journal of Thermal Sciences,* Vol. 145, pp. 105984.

Lui, C.H., Fong, N.K., Bejan, A. and Lorente, S. and Chow, W.K., 2015. "Constructal design of evacuation from a three-dimensional living space". *Physica A,* Vol. 422, pp. 47-57.

Moraga, N.O., Marambio, M.A., Cabrales, R.C., 2017. "Geometric multigrid technique for solving heat convection-diffusion and phase change problems". *International Communications of Heat and Mass Transfer,* Vol. 88, pp. 108–119.

Nithyadevi, N., Begum, A.S., Oztop, H.F. and Abu-Hamdeh, N., 2017. "Mixed convection analysis in heat transfer enhancement of a nanofluid filled porous enclosure with various wall speed ratios". *International Journal of Heat and Mass Transfer,* Vol. 113, pp. 716–729.

Razera, A.L., da Fonseca, R.J.C., Isoldi, L.A., dos Santos, E.D., Rocha, L.A.O. and Biserni, C., 2018. "Constructal design of a semi-elliptical fin inserted in a lid-driven square cavity with mixed convection". *International Journal of Heat and Mass Transfer,* Vol. 126, pp. 81-94.

Rodrigues, P.M., Biserni, C., de Escobar, C.C., Rocha, L.A.O., Isoldi, L.A. and dos Santos, E.D., 2020. "Geometric optimization of a lid-driven cavity with two rectangular intrusions under mixed convection heat transfer: A numerical investigation motivated by constructal design". *International Communications of Heat and Mass Transfer,* Vol. 117.

## 7. RESPONSIBILITY NOTICE

The authors are the only responsible for the printed material included in this paper.